

# Characterization of BaTiO<sub>3</sub> Powders and Ceramics Prepared Using the Sol-gel Process, with Triton X-100 Used as a Surfactant

Cheng-cheng Zheng, Bin Cui\*, Qiao-ming You, Zhu-guo Chang

Key Laboratory of Synthetic and Natural Functional Molecule Chemistry (Ministry of Education)

Northwest University

Xi'an, P. R. China

zhengccdyx@163.com; cuibin@nwu.edu.cn; youchem\_2008@126.com; chang1960zg1960@163.com

**Abstract:** We prepared BaTiO<sub>3</sub> xerogels, powders, and ceramics using the sol-gel process, with Triton X-100 used as a surfactant. We then characterized these materials by means of thermogravimetric, differential scanning calorimetry, Fourier-transform infrared, X-ray diffraction, and transmission and scanning electron microscope analysis, and investigated the dielectric properties of the resulting ceramics. The powders calcined at 800 °C for 2 h were mainly the BaTiO<sub>3</sub> phase, which contained a small amount of BaCO<sub>3</sub>. With increasing concentration of Triton X-100, the particle size of the powders decreased and their dispersion improved. The BaTiO<sub>3</sub> particle size ranged between 30 and 70 nm. After sintering, the content of the tetragonal BaTiO<sub>3</sub> phase increased with increasing surfactant concentration. The average grain size of the ceramics increased from 0.6 to 3.0 μm as the [Triton X-100]/[Ti(OC<sub>4</sub>H<sub>9</sub>)<sub>4</sub>] ratio increased from 0 to 1:8. Moreover, the room-temperature permittivity values were all greater than 3000. The ceramic produced with a [Triton X-100]/[Ti(OC<sub>4</sub>H<sub>9</sub>)<sub>4</sub>] ratio of 1:16 had the maximum room-temperature permittivity (4881).

**Keywords:** ceramics; BaTiO<sub>3</sub>; surfactant; sol-gel method; dielectric constant

\* Corresponding author. Tel.: +86-029-8830-2604; fax: +86-029-8830-3798.

## 1. Introduction

Barium titanate is a good candidate for a variety of applications due to its excellent dielectric, ferroelectric, and piezoelectric properties. As materials science has developed more advanced techniques, the ceramics prepared with barium titanate (BaTiO<sub>3</sub>) powders have been endowed with many beneficial characteristics, such as smaller grain size, fewer agglomerations, and a higher dielectric constant. The preparation methods significantly influence the structure and properties of these materials [1]. Therefore, finding ways to optimize these methods has attracted increasing attention.

Traditionally, BaTiO<sub>3</sub> has been prepared using solid-state reactions between the constituent oxides and carbonates at a temperature above 1000 °C. The particle size and purity of the raw materials prepared by this method seriously affect the dielectric properties; nonhomogeneous powders can seriously degrade product performance. Recently, more and more researchers have investigated wet chemistry methods [2], such as the hydrothermal [3], precipitation [4], micro-emulsion [5], and sol-gel [6] methods. The sol-gel process has been intensively studied because it facilitates the preparation of powders with high purity, small grain size, and good uniformity. However, the BaTiO<sub>3</sub> powders with smaller grain size pre-

pared using the sol-gel process have high chemical reactivity, and thus, they easily agglomerate. This suggests that a surfactant is necessary to prevent agglomeration of these particles. Peng fei Yu et al. [7] prepared BaTiO<sub>3</sub> powders with good dispersion using oil acid as surfactant. The maximum room temperature permittivity they achieved was 4569, which was approximately 2000 higher than the ceramics prepared using traditional solid-state methods. However, ceramics with a higher permittivity value would be desirable, so research continued in an effort to identify a more effective surfactant. Triton X-100 is often used to form microemulsions that can prevent the agglomeration of particles. The particle size can then be controlled by adjusting the size of microcapsules. Tian Ma et al. [8] prepared well-dispersed ZrO<sub>2</sub> using Triton X-100 as a surfactant, and the resulting powders had a high sintering activity. Angshuman Pal et al. [9] successfully synthesized monodispersed Pt nanoparticles using Triton X-100 as surfactant.

In the present study, we investigated the possibility of obtaining a better dispersion of BaTiO<sub>3</sub> nanoparticles and finer-grained ceramics with a higher dielectric constant using the sol-gel method, with Triton X-100 used as a surfactant. To our knowledge, this approach has not been reported previously. Based on the results of our study, we discuss the mechanisms by which Triton X-100 influences the phase compositions and morphologies of the BaTiO<sub>3</sub> powders and the microstructures of the resulting

Project supported by the National Natural Science Foundation of China (Grant No. 21071115); The Science Research and Project Program of the Education Committee of Shaanxi Province (No. 09JC01).

BaTiO<sub>3</sub> ceramics. We also discuss the dielectric properties of these ceramics.

## 2. Experimental

### 2.1. Chemicals and equipment

The Ti(OC<sub>4</sub>H<sub>9</sub>)<sub>4</sub>(Ti(OBu)<sub>4</sub>), Ba(CH<sub>3</sub>COO)<sub>2</sub>(Ba(Ac)<sub>2</sub>), and Triton X-100 used in this study were all reagent-grade, and were made in China. Measurement of the properties of the xerogel, [Triton X-100]/[Ti(OBu)<sub>4</sub>] at a ratio = 1:8, was performed by means of thermogravimetric (TG) and differential scanning calorimetry (DSC) measurements using an SDT Q600 thermal analyzer (TA Instruments) at temperatures ranging from 20 to 1000 °C (at 10 °C/min) with a nitrogen atmosphere. We determined the phase composition of the BaTiO<sub>3</sub> powders and ceramics by means of X-ray diffraction (XRD; D8 Advanced, Bruker, Frankfurt, Germany). We observed the morphology of the powders using an H-600 transmission electron microscope (TEM; Hitachi, Japan). We observed the microstructure of the as-sintered ceramics using an S-570 scanning electron microscope (SEM; Hitachi). We measured the dielectric properties of the ceramics using an HP 4284A LCR meter (Hewlett-Packard, America) controlled by a computer at 1 kHz, with the testing temperature controlled by high and low gimbals (GDW-100E, China) between -30 and 140 °C.

### 2.2. Preparation

We synthesized the BaTiO<sub>3</sub> powders using the sol-gel process, with Triton X-100 used as a surfactant. Ti(OBu)<sub>4</sub> and Ba(Ac)<sub>2</sub> were used as the starting materials. Glacial acetic acid was added to the Ti(OBu)<sub>4</sub>, then Triton X-100 and absolute ethanol were added to the mixture, with a [Triton X-100]/[Ti(OBu)<sub>4</sub>] ratio ranging between 0 and 1:8. We prepared an aqueous Ba(Ac)<sub>2</sub> solution by dissolving Ba(Ac)<sub>2</sub> in distilled water. We then added the Ba(Ac)<sub>2</sub> solution into the previously mixed solution to form the BaTiO<sub>3</sub> precursor. The molar ratio of Ba and Ti was controlled at 1:1.

The BaTiO<sub>3</sub> precursor was stirred vigorously for 30 min, with gelling at room temperature, and the xerogels were obtained by drying at a temperature of 70 to 80 °C. We obtained the BaTiO<sub>3</sub> powders by calcining at 800 °C for 2 h. We chose this temperature and duration based on preliminary testing (data not shown) that revealed a high yield under these conditions. The as-prepared powders were then ball-milled for 12 h in a polyethylene bottle using zirconia balls, with ethyl alcohol as the medium. We then compressed the dried slurry into discs 12 mm in diameter at around 6 MPa and sintered the discs at 1250 °C for 2 h. After coating both sides of the sintered discs with silver paste, we measured the dielectric properties of

the ceramics.

## 3. Results and discussion

### 3.1. Thermal analysis of the xerogel

Fig. 1 shows the TG and DTG curves during the thermal decomposition process of the BaTiO<sub>3</sub> xerogel. As shown by the TG curve, the total weight loss was approximately 43.6% and the process could be divided into four steps. First, residual water and organic solvents vaporize, with a weak weight loss at a temperature below 200 °C. Second, between 200 and 400 °C, the weight loss increases (with a DTG peak at 318 °C); this can be attributed to the decomposition of Ba(Ac)<sub>2</sub> to form BaCO<sub>3</sub> and organic compounds. The Triton X-100 probably decomposes during this step due to its structure and its low boiling point (270 °C). Third, the complete decomposition of the residual organic compounds occurs between 600 and 680 °C, with a DTG peak at around 657 °C. Finally, BaCO<sub>3</sub> reacts with TiO<sub>2</sub> to form BaTiO<sub>3</sub> between 700 and 780 °C, with a DTG peak around 730 °C. The process of BaTiO<sub>3</sub> formation was further investigated by analysis of the Fourier-transform infrared (FT-IR) spectra and IR patterns for xerogels calcined at different temperatures for 2 h; results are presented in section 3.2.

Fig. 2 shows the DSC curve during the thermal decomposition process of the BaTiO<sub>3</sub> xerogel. The DSC curve confirmed the results shown in the TG curve. The BaTiO<sub>3</sub> forms as a result of the reaction between BaCO<sub>3</sub> and TiO<sub>2</sub>, with an endothermic peak at about 732 °C in the DSC curve. There is also a broad peak at temperatures higher than 800 °C. This suggests the occurrence of a phase transition from a cubic to a tetragonal phase. We tested this hypothesis using XRD analysis (section 3.3).

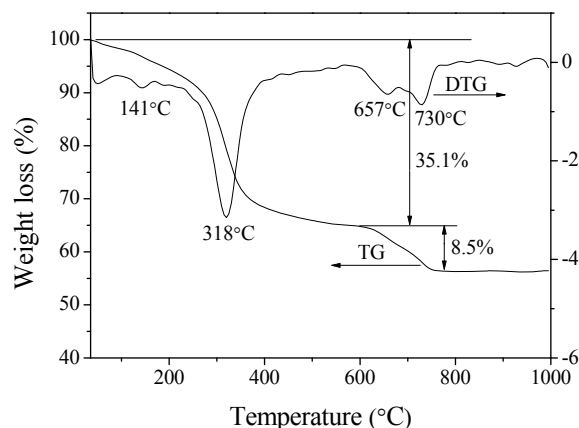


**Figure 1.** TG and DTG curves during the thermal decomposition process of BaTiO<sub>3</sub> xerogel prepared with a [Triton X-100]/[Ti(OBu)<sub>4</sub>] ratio of 1:8.

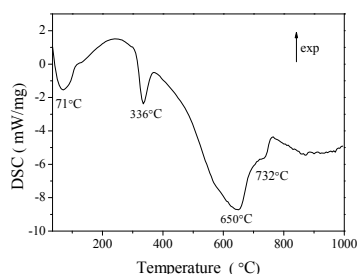


Figure 2. DSC curve for the thermal decomposition of BaTiO<sub>3</sub> xerogel prepared with a [Triton X-100]/[Ti(OBu)<sub>4</sub>] ratio of 1:8.

### 3.2. FT-IR spectra analysis

Fig. 3 shows the FT-IR patterns for xerogels calcined at different temperatures. Line a in Fig. 3 shows doublet absorption at about 1420.0 and 1569.2 cm<sup>-1</sup>, which represent the symmetric [vs(COO<sup>-</sup>)] and asymmetric [vas(COO<sup>-</sup>)] stretching vibrations, respectively. When the xerogel was calcined at 400 °C for 2 h, the COO<sup>-</sup> absorption disappeared and CO<sub>3</sub><sup>2-</sup> absorption could be observed at about 1433.1 cm<sup>-1</sup> as a result of the symmetric [vs(CO<sub>3</sub><sup>2-</sup>)] stretching vibration. These results suggest that acetates are transformed into carbonates as the calcining temperature increases. When the temperature increased further, the intensity of the absorption peak decreased because of the reaction between BaCO<sub>3</sub> and TiO<sub>2</sub>. When the xerogel was calcined at 900 °C for 2 h, the CO<sub>3</sub><sup>2-</sup> absorption was no longer observed.

### 3.3. XRD patterns of the xerogels at different heat treatment temperatures

Fig. 4 shows the XRD spectra for xerogels calcined at different temperatures for 2 h. The XRD results confirm the TG and FT-IR results. When the temperature was 250 °C or less, diffraction peaks for Ba(Ac)<sub>2</sub> (PDF #26-0130) are observed (lines a and b). When the xerogel was calcined at 400 °C for 2 h, Ba(Ac)<sub>2</sub> is transformed into BaCO<sub>3</sub> (PDF #41-0373). BaTiO<sub>3</sub> formed after calcining at 700 °C for 2 h. There were also some peaks for BaCO<sub>3</sub>,

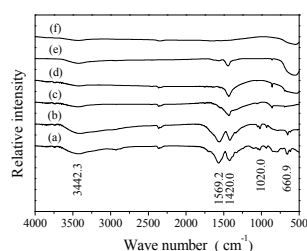


Figure 3. FT-IR spectra for xerogels calcined at different temperatures for 2 h. (a) 70 °C; (b) 250 °C; (c) 400 °C; (d) 700 °C; (e) 800 °C; (f) 900 °C.

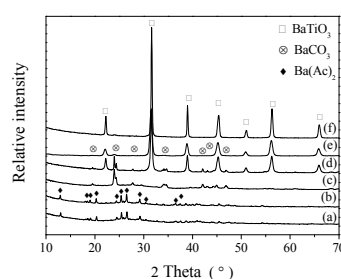


Figure 4. XRD patterns for xerogels calcined at different temperatures for 2 h. (a) 70 °C; (b) 250 °C; (c) 400 °C; (d) 700 °C; (e) 800 °C; (f) 900 °C.

and the intensity of these peaks decreased with increasing temperature. When the xerogel was calcined at 800 °C for 2 h, BaTiO<sub>3</sub> (PDF #05-0626) formed.

### 3.4. Phase composition and microstructure of the BaTiO<sub>3</sub> powders

Fig. 5 shows the XRD patterns of the BaTiO<sub>3</sub> powders calcined at 800 °C for 2 h with different [Triton X-100]/[Ti(OBu)<sub>4</sub>] ratios. The BaTiO<sub>3</sub> phase is mainly cubic (PDF #31-0174) in all samples, with a small amount of BaCO<sub>3</sub> (PDF #45-1471). As the [Triton X-100]/[Ti(OBu)<sub>4</sub>] ratio increased, the amount of impurities first increased, and then decreased. The estimated grain size of the BaTiO<sub>3</sub> powders decreased to 29.2, 27.1, 27.0, 25.9 and 23.4 nm, respectively, for ratios of 0, 1/64, 1/32, 1/16 and 1/8 based on Scherrer's formula ( $D = k\lambda/\beta\cos\theta$ ).

Fig. 6 shows TEM micrographs of the BaTiO<sub>3</sub> powders, which show the average size of the particles in the powders. The particle size obviously decreases with increasing amounts of Triton X-100. The size of the particles in the powders averaged 65, 56, 48, 46, and 37 nm for ratios of 0, 1/64, 1/32, 1/16, and 1/8, respectively. The dispersion also improved with increases in the ratio. This results from the formation of the microcapsules, which can prevent the agglomeration of particles in the

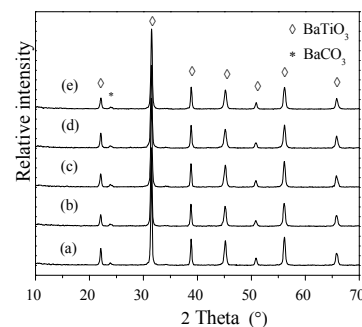
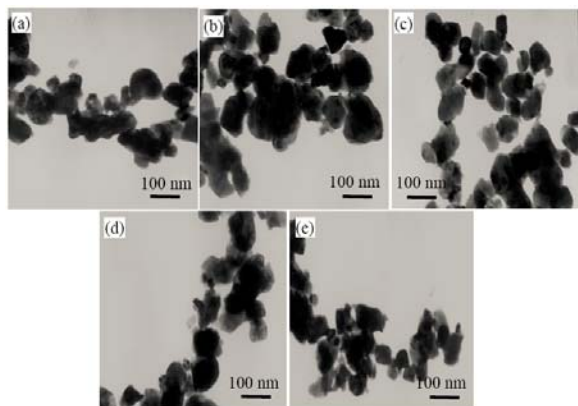


Figure 5. XRD patterns of the BaTiO<sub>3</sub> powders prepared by calcining xerogels at 800 °C for 2 h with different [Triton X-100]/[Ti(OBu)<sub>4</sub>] ratios: (a) 0; (b) 1:64; (c) 1:32; (d) 1:16; (e) 1:8.

(e) 1:8.



**Figure 6.** TEM micrographs of the BaTiO<sub>3</sub> powders prepared by calcining xerogels at 800 °C for 2 h with different [Triton X-100]/[Ti(OBu)<sub>4</sub>] ratios: (a) 0; (b) 1:64; (c) 1:32; (d) 1:16; (e) 1:8.

powders. The size of the microcapsules becomes smaller with increasing surfactant concentration, leading to the production of smaller particles. However, when the xerogels were calcined at 800 °C, it was easier for the smaller particles to agglomerate because of their higher surface energy. Therefore, when the amount of Triton X-100 is higher than a certain value, the dispersion of particles in the powders decreases.

The amount of Triton X-100 strongly affects the phase composition and microstructures of the products. This results from the formation of microcapsules as a result of the effects of Triton X-100. Some metal ions will precipitate and coat the surface of the microcapsules. Therefore, Ba(Ac)<sub>2</sub> is observed in lines a and b of Fig. 4. The microcapsules do not form in a system without Triton X-100. Barium ions are homogeneously bounded by the network structure of the Ti colloid, which promotes the reaction between BaCO<sub>3</sub> and TiO<sub>2</sub>. Therefore, the XRD patterns show a slight increase in the amount of BaCO<sub>3</sub> as the [Triton X-100]/[Ti(OBu)<sub>4</sub>] ratio increases. With an increasing [Triton X-100]/[Ti(OBu)<sub>4</sub>] ratio, the microcapsules have a smaller volume and result in particles with a smaller size. On the one hand, the small microcapsules can increase precipitation of metal ions. This impedes the formation of BaTiO<sub>3</sub>. On the other hand, the small microcapsules promote the reaction between BaCO<sub>3</sub> and TiO<sub>2</sub>. The XRD patterns show that the amount of impurity initially increases, and then decreases, with increasing amounts of surfactant. The decreased size of the particles in the powders can therefore be attributed to the smaller microcapsule size.

### 3.5. Phase composition, microstructure, and dielectric properties of the BaTiO<sub>3</sub> ceramics

We prepared the ceramics by sintering at 1250 °C for 2 h. Fig. 7 shows the XRD patterns of the ceramics. The peaks at around 45° split increasingly obviously with

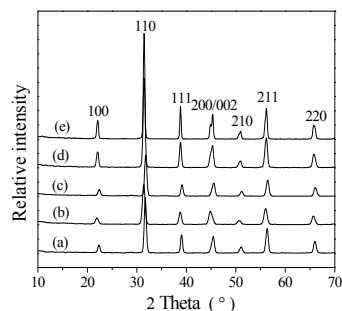


**Figure 7.** XRD patterns of the BaTiO<sub>3</sub> ceramics calcined at 800 °C for 2 h and sintered at 1250 °C for 2 h at different [Triton X-100]/[Ti(OBu)<sub>4</sub>] ratios: (a) 0; (b) 1:64; (c) 1:32; (d) 1:16; (e) 1:8.

increasing surfactant ratios. This indicates that the content of the tetragonal BaTiO<sub>3</sub> phase increased. Fig. 8 shows the SEM micrographs of the ceramics, and Table 1 summarizes their key properties. The grain size increased with increasing surfactant ratios. The grain size of the ceramics prepared using small barium titanate particles was larger than that of ceramics prepared using large particles. This results from grain growth processes that are dominated by pore drag. When the green body has a density similar to 90% during the sintering process, the growth rate of grains formed from small particles is higher than that of grains formed from large particles. The particles that initially have a small size have a lower activation energy for grain growth [10-13]. Fig. 8 also shows that the porosity decreases with decreasing particle size. The powders with small particles have a higher surface energy, which is beneficial for increasing the density of the resulting ceramics.

Fig. 9 shows the temperature dependence of the permittivity for the ceramics, whose dielectric properties are summarized in Table 1. The dielectric constants at

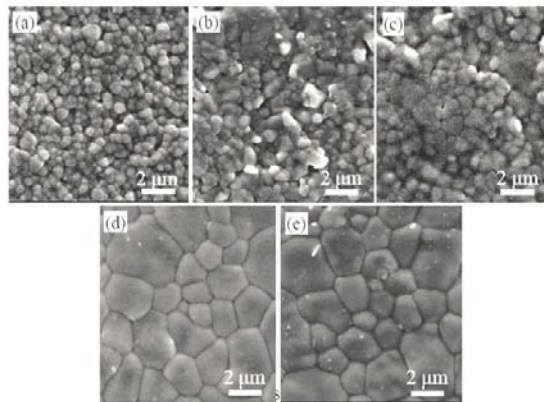


**Figure 8.** SEM micrographs of the BaTiO<sub>3</sub> ceramics calcined at 800 °C for 2 h and sintered at 1250 °C for 2 h at different [Triton X-100]/[Ti(OBu)<sub>4</sub>] ratios: (a) 0; (b) 1:64; (c) 1:32; (d) 1:16; (e) 1:8.

**Table 1.** Density, grain size, and dielectric properties of the ceramics calcined at 800 °C for 2 h and sintered the ceramics at 1250 °C for 2 h at different [Triton X-100]/[Ti(OBu)<sub>4</sub>] ratios.

[Triton X-100]/[Ti(OBu) <sub>4</sub> ] ratio	Relative theoretical density (%)	Average grain size (μm)	ε (25 °C)	tanδ (25 °C)
0	95.7	0.6	3666	0.018
1:64	95.8	0.8	4387	0.026
1:32	95.6	0.9	4806	0.038
1:16	95.4	2.5	4881	0.037
1:8	96.1	3.0	4381	0.032

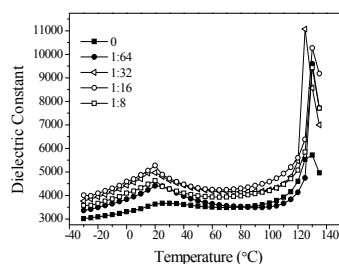


**Figure 9.** Temperature dependence of the permittivity of the ceramics calcined at 800 °C for 2 h and sintered at 1250 °C for 2 h at different [Triton X-100]/[Ti(OBu)<sub>4</sub>] ratios.

room temperature initially increase with an increasing surfactant ratio, and then decrease. This result agrees with the suggestions of Pedro Duran et al.<sup>[14]</sup>, who suggested that the critical grain size was around 1 μm. Ceramics with a grain size of about 1 μm have the maximum permittivity at room temperature. Therefore, the ceramics with grain sizes of 0.9 and 2.5 μm in the present study had the highest dielectric constants at room temperature (Table 1) because they were closest to 1 μm in diameter. This behavior was attributed to the domain size effect or to a change in the ferroelectric structure of the material [14]. A grain size below 0.5 μm, with a probable cubic structure, would have a lower dielectric constant. Fig. 8(a, b, and c) shows the presence of some small grains, and that the content of the tetragonal BaTiO<sub>3</sub> phase increases with increasing grain size. Therefore, the ceramic produced with a [Triton X-100]/[Ti(OBu)<sub>4</sub>] ratio of 1:16, with a grain size of 2.5 μm, had the maximum permittivity (4881) and nearly the maximum dielectric loss (0.037).

#### 4. Conclusions

(1) We produced BaTiO<sub>3</sub> powders with a [Triton X-100]/[Ti(OBu)<sub>4</sub>] ratio ranging from 0 to 1:8 using the sol-gel process, with [Triton X-100] used as a surfactant. The size of the nanosize particles in the powders calcined at 800 °C ranged from 30 to 70 nm. The dispersion of the powders was improved by the formation of microcapsules.

(2) After sintering the ceramic, the content of the tetragonal BaTiO<sub>3</sub> phase increased and the porosity decreased with an increasing surfactant ratio. The average grain size increased as the [Triton X-100]/[Ti(OBu)<sub>4</sub>] ratio increased from 0 to 1:8. This resulted from grain growth dominated by pore drag.

(3) The ceramic with a [Triton X-100]/[Ti(OBu)<sub>4</sub>] ratio of 1:16 that was calcined at 800 °C for 2 h and then sintered at 1250 °C for 2 h had the maximum room-temperature dielectric constant (4881), and nearly the maximum dielectric loss (0.037).

#### 5. Acknowledgment

This work was supported by the National Natural Science Foundation of China (Grant No. 21071115) and the science research and project program of the education committee of Shaanxi Province (No. 09JC01).

#### References

- [1] V. Brizé, G. Gruener, K. Wolfman, K. Fatyeyeva, M. Tabellout, M. Gervais and F. Gervais, "Grain size effects on the dielectric constant of CaCu<sub>3</sub>Ti<sub>4</sub>O<sub>12</sub> ceramics," *Mater. Sci. Eng.*, vol. B129, pp. 135–138, April 2006.
- [2] W. Lu, M. Quilitz, and H. Schmidt, "Nanoscaled BaTiO<sub>3</sub> powders with a large surface area synthesized by precipitation from aqueous solutions: Preparation, characterization and sintering," *J. Eur. Ceram. Soc.*, vol. 27, pp. 3149–3159, February 2007.
- [3] A. Pal, S. Shah, S. Belochapkine, D. Tanner, E. Magner, and S. Devi, "Room temperature synthesis of platinum nanoparticles in water-in-oil microemulsion," *Colloids Surf.*, vol. A337, pp. 205–207, April 2009.
- [4] W. Widiyastuti, S. Y. Lee, F. Iskandar, and K. Okuyama, "Sintering behavior of spherical aggregated nanoparticles prepared by spraying colloidal precursor in a heated flow," *Adv. Powder Technol.*, vol. 20, pp. 318–326, July 2009.
- [5] Y. Wang, G. Xu, L. Yang, Z. H. Ren, X. Wei, W. J. Weng, P. Du, G. Shen, and G. R. Han, "Hydrothermal synthesis of single-crystal BaTiO<sub>3</sub> dendrites," *Mater. Lett.*, vol. 63, pp. 239–241, January 2009.
- [6] R. Kaviani, and A. Saidi, "Sol-gel derived BaTiO<sub>3</sub> nanopowders," *J. Alloys Compd.*, vol. 468, pp. 528–532, January 2009.
- [7] P. Yu, B. Cui, and Q. Shi, "Preparation and characterization of BaTiO<sub>3</sub> powders and ceramics by sol-gel process using oleic acid as surfactant," *Mater. Sci. Eng.*, vol. A473, pp. 34–41, January 2008.
- [8] T. Ma, Y. Huang, J. Yang, J. He, and L. Zhao, "Preparation of spherical zirconia powder in microemulsion system and its densification behavior," *Mater. Des.*, vol. 25, pp. 515–519, September 2004.
- [9] X. Wu, L. Zou, S. Yang, and D. Wang, "Structural Characterizations of Organo-Capped Barium Titanate

- Nanoparticles Prepared by the Wet Chemical Route,” *J. Colloid Interface Sci.*, vol. 239, pp. 369–373, 369–373, July 2001.
- [10] M. Mazaheri, A. Simchi, M. Dourandish, and F. Golestani-Fard, “Master sintering curves of a nanoscale 3Y-TZP powder compacts,” *Ceram. Int.*, vol. 35, pp. 547–554, March 2009.
- [11] Y. Sakabe, Y. Yamashita, and H. Yamamoto, “Dielectric properties of nano-crystalline BaTiO<sub>3</sub> synthesized by micro-emulsion method,” *J. Eur. Ceram. Soc.*, vol. 25, pp. 2739–2742, April 2005.
- [12] J. Kanters, U. Eisele, and J. Roedel, “Effect of initial grain size on sintering trajectories,” *Acta Mater.*, vol. 48, pp. 1239–1246, April 2000.
- [13] P. Duran, D. Gutierrez, J. Tartaj, and C. Moure, “Densification behaviour, microstructure development and dielectric properties of pure BaTiO<sub>3</sub> prepared by thermal decomposition of (Ba,Ti)-citrate polyester resins,” *Ceram. Int.*, vol. 28, pp. 283–292, March 2002.
- [14] M. M. Vijatović, J. D. Bobić, and B. D. Stojanović, “History and challenges of barium titanate: Part I,” *Sci. Sintering*, vol. 40, pp. 155–165, March 2008.